Search for a Stochastic Gravitational-wave Background with Torsion-bar Antennas

Ayaka Shoda[1], Masaki Ando[2], Kenshi Okada[1], Koji Ishidoshiro[3], Wataru Kokuyama[1], Yoichi Aso[1], Kimio Tsubono[1]

[1]Department of Physics, The University of Tokyo, Bunkyo-ku, Tokyo 113-0033, Japan
[2]Department of Physics, Kyoto University, Kitashirakawa Oiwake-cho, Sakyo-ku, Kyoto 606-8502, Japan
[3]Institute of Particle and Nuclear Studies, High Energy Accelerator Research Organization (KEK), 1-1 Oho, Tsukuba, Ibaraki 305-0801, Japan

E-mail: shoda@granite.phys.s.u-tokyo.ac.jp

Abstract. We performed the simultaneous observational run and searched for a stochastic gravitational waves (GW) background with prototypes of Torsion-bar Antenna (TOBA). TOBA is a new GW detector which consists of test mass bars which rotate by ~~the~~ tidal force from GWs and fundamentally has a good sensitivity at lower frequencies, such as 0.1 – 1.0 Hz. The prototype has a 20-cm test mass bar which is levitated by the pinning effect of a superconductor. The data was taken from 1:00 am to 10:00 am on March 11th 2011, at Tokyo and Kyoto in Japan. As a result, we did not detect a stochastic GW background with false alarm rate of 5 %, and set an upper limit on a stochastic GW background ~~whose power spectrum density is assumed to be proportional to f^{-3}~~. Our 95 % confidence upper limit is $\Omega_{\rm gw}h_0^2 < 1.2 \times 10^{19}$ at 0.06 – 0.9 Hz, where $\Omega_{\rm gw}$ is the GW energy density per logarithmic frequency interval in units of the critical density and h_0 is the Hubble constant per 100 km/sec/Mpc. We had established the simultaneous observation ~~system~~ and the analysis pipeline with TOBAs, and set an upper limit at a wider frequency band. ~~we are planning to perform the additional simultaneous observational run in order to derive a better upper limit.~~

1. Introduction

Recently, many gravitational wave (GW) detectors have been developed. GWs have not been detected yet, but when they are detected, they will provide us new aspects of universe. Especially, a stochastic GW background is a cosmologically interesting target. It will provide us much information about phenomena occurred in the universe shortly after its birth, such as the inflation. Therefore, it has been eagerly searched for with a number of experiments.

~~For example,~~ the ground-based laser interferometer GW detectors, LIGO [1] and Virgo [2], have set a 95 % confidence upper limit on a stochastic GW background of in the frequency band around 100 Hz [3]. ~~In addition,~~ a pair of synchronous recycling interferometers set an upper limit at 100 MHz [4]~~, and the~~ cryogenic bar detectors, Explorer and Nautilus, have done at 907 Hz [5]. At much lower frequency band, the Doppler tracking with the Cassini spacecraft at 10^{-6} – 10^{-3} Hz [6], the pulsar timing by PSR B1855+09 at 10^{-9} – 10^{-7} Hz [**?**], and measurement of cosmic microwave background has established an upper limit at 10^{-18} – 10^{-16} Hz [**?**][8].

So far, no upper limit had been set at 0.01 – 1 Hz. The space GW detectors, LISA [9] and DECIGO [10], are planned to be launched and explore this frequency band. However, it is very

challenging to launch more than three satellites and construct laser interferometer between the satellites.

Then, we designed a novel GW detector, "Torsion-bar Antenna", called TOBA [11]. It is fundamentally sensitive to GWs below 1 Hz even on the ground. We have already developed prototypes of TOBA with one 20-cm long test mass bar. By a single prototype TOBA, the first upper limit on a stochastic GW background had been set at 0.2 Hz [12].

However, it is difficult to judge that stochastic GW background is present by a single detector. We can mention about the presence of a stochastic GW background only if the signal exceeds the expected noise level. Therefore, the method of two-detector correlation is important in order to search ~~for~~ a stochastic GW background. In this paper, we report simultaneous observational run performed at Tokyo and Kyoto in Japan and cross correlation analysis with two prototypes of TOBA. Here we demonstrated the two-detector correlation with TOBA and evaluate the its capabilities for low-frequency GW observations.

2. Torsion-bar Antenna

2.1. Principle of Torsion-bar Antenna

TOBA has two test mass bars suspended at their center. (See figure 1.) When they are arranged orthogonal to each other, the bars rotates differentially by the tidal force from GWs. ~~And~~ their differential angular fluctuation is monitored by laser interferometric sensors.

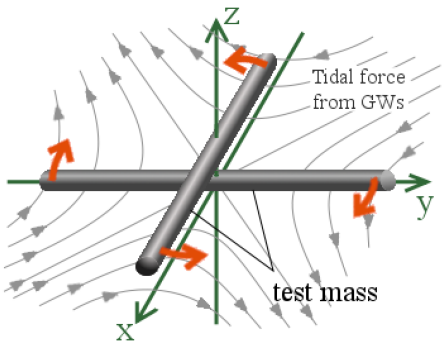

Figure 1. A conceptual drawing of TOBA.

Let us consider a test mass bar is arranged along x axis, and suspended so that they rotate around the z axis. (Figure 1.) When the GW come along z axis, the bars are affected by the tidal force from GWs. The angular fluctuation θ obeys the equation of motion:

$$I\ddot{\theta} + \gamma\dot{\theta} + \kappa\theta = F_{\rm gw}(t) \tag{1}$$

where I is the moment of inertia of the test mass, γ and κ are the damping constant and the spring constant around z axis, and $F_{\rm gw}$ is the torque caused by the GW. Assuming that the antenna is smaller enough than the wavelength of the GW, and that GW has $\times$-polarization, the angular fluctuation is simply represented as

$$\tilde{\theta}(f) = \frac{q_\times}{2I}\tilde{h}_\times(f) \tag{2}$$

above the resonant frequency $= 1/(2\pi)\sqrt{\kappa/I}$, where $q_\times = q_{12} = q_{21}$ is the dynamic quadrupole moment of the test mass, and $h_\times$ is the amplitude of the $\times$-polarized GW [11]. ~~Note that it is assumed that the test mass bar is thin enough.~~

The fact that a TOBA is sensitive to GWs above its resonant frequency is the same as laser interferometric GW antennas, which have test mass mirrors suspended as pendulums. The point is that the resonant frequency in the rotational degree of freedom is on the order of a few mHz while the resonant frequency of the pendulum is around 1 Hz. This is the reason that a TOBA is fundamentally sensitive to GWs below 1 Hz even on the ground.

2.2. Prototype Torsion-bar Antenna

We have developed prototypes of TOBA. Pictures of the prototype TOBA is shown in figure 2.

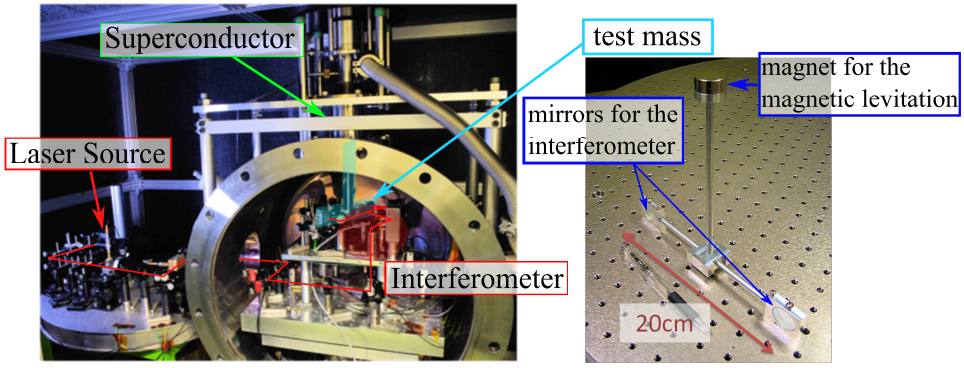

Figure 2. Pictures of the prototype TOBA.

a

It has a 20-cm test mass bar, which is levitated by the flux spinning effect of ~~the~~ superconductor. This magnetic suspension let the test mass free to rotate while it provide large suspension force. In this case, its rotational resonance frequency is about 5 mHz.

The rotation of the test mass bar is read by a laser Michelson interferometer. A las laser source wavelength of 1064 nm and output power of 40 mW. The beam goes to the mirrors attached at the both ends of the test mass, thus the differential ~~between~~ two beam path length is proportional to the rotation angle.

change in the

The test mass is controlled by coil-magnet actuators. To compose the actuators, the test mass has two magnets of ϕ1 mm at the each end of the arm. bar

We have almost the same prototype TOBAs at University of Tokyo and Kyoto University. We performed simultaneous observational run with them.

3. Observation

~~We performed simultaneous observational run with the prototype TOBAs since the two-detector correlation is effective in searching for a stochastic GW background.~~

The observation is performed from 1:00 am – 10:00 am at March 11, 2011 at Tokyo and Kyoto in Japan. The latitude and longitude of Tokyo is 35.71° N and 139.76° E, and of Kyoto is 35.03° N and 135.78° E. The ~~site in Tokyo~~ is about 370 km far from the cite of Kyoto. (See figure 3) The both test mass bars are oriented to the north-to-south direction. An overlap reduction function which represents the difference of the response to GWs between two detectors is shown in figure 4. Note that the overlap reduction function of two TOBAs is calculated in the same way as two interferometers since the antenna pattern of TOBA is the same. At lower frequency than 1 Hz, the overlap reduction function is almost one, which means that the two detectors respond to GWs almost equally.

We recorded GPS signal to adjust time shift between the both site as well as feedback signal and error signal. We also used the on-line calibration signal which is 8.7 Hz sine wave in order to

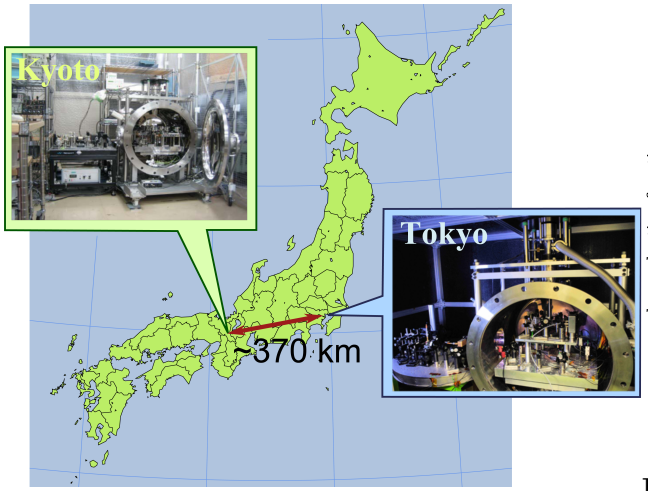

Figure 3. The location of Tokyo and Kyoto in Japan.

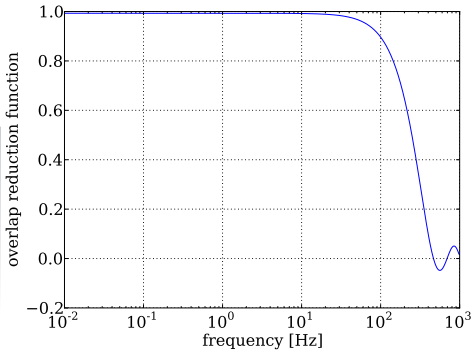

Figure 4. The overlap reduction function of two prototypes of TOBA at Tokyo and Kyoto.

monitor the fluctuation of the control open-loop gain. The on-line calibration signal is injected into the feedback signal, and the real-time gain is calculated by comparing signal before the injection and signal after the injection.

The equivalent strain noise spectra of two detectors are shown in fig 5. Their sensitivity is limited by the seismic noise at higher frequency than 0.1 Hz, and by the magnetic coupling noise at lower frequency than 0.1 Hz [12, 13].

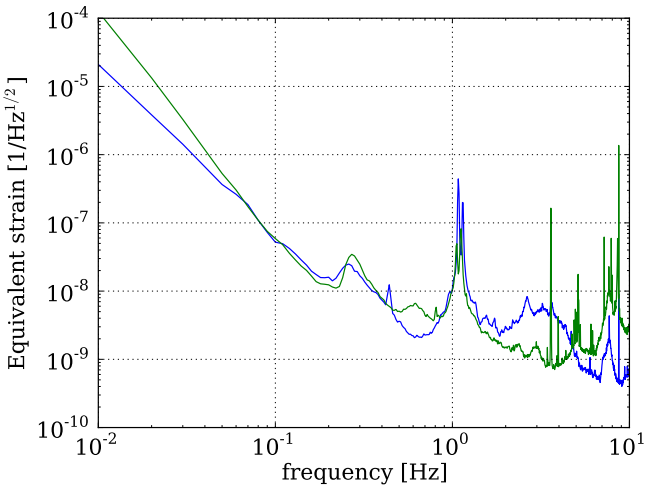

Figure 5. The equvalent strain noise spectra of two detectors. Blue line is the strain of the detector in Tokyo, and green line is the strain of the detector in Kyoto.

4. Analysis

4.1. A spectrum of a stochastic gravitational wave background

Our target, a stochastic GW background, is considered to be a superposition of GWs from astrophysical sources and from cosmological sources. Therefore, we cannot predict its waveform.

Here, we assume that the amplitude of a stochastic GW background h_{ij} has random variables, and we characterize the amplitude by its ensemble average of power spectrum density (PSD) $S_{\rm gw}(f)$ written as

$$S_{\rm gw}(f) = \frac{3H_0^2}{10\pi^2} f^{-3}\Omega_{\rm gw}(f). \tag{3}$$

Here, H_0 is the Hubble constant [14], and $\Omega_{\rm gw}(f)$ is defined as

$$\Omega_{\rm gw}(f) = \frac{f}{\rho_c}\frac{d\rho_{\rm gw}}{df}, \tag{4}$$

where $\rho_c = 3c^2H_0^2/8\pi G$ is the critical energy density of the universe and $\rho_{\rm gw} = (c^2/32\pi G)\langle \dot{h}_{ij}\dot{h}^{ij}\rangle$ is the gravitational-wave energy density [7].

Also, a stochastic GW background is assumed to be stationary, unpolarized, and isotropic.

4.2. The principle of the cross correlation analysis

The equivalent strain output $s_i(t)$ is written as

$$s_i(t) = n_i(t) + h_i(t), \tag{5}$$

where i donates the index of the two detectors. $n_i(t)$ and $h_i(t)$ is the detector's noise in equivalent strain and the signal due to a stochastic GW background. The cross correlation between the two outputs is

$$\begin{aligned} Y &= \int_{-T/2}^{T/2} dt \int_{-T/2}^{T/2} dt' s_1(t)s_2(t')Q(t-t') \\ &\sim \int_{-\infty}^{+\infty} df \tilde{s}_1^*(f)\tilde{Q}(f)\tilde{s}_2(f), \end{aligned} \tag{6}$$

where T is the observation time and $Q(t)$ is a real filter function called an optimal filter, which is decided so that signal-to-noise ratio is maximized. Here we assume that T is long enough to be approximated as $T \to +\infty$ and that $Q(t)$ converges on 0 when t is large. Note that the integrated interval has to be restricted for the analysis with the actual discrete output data.

The signal-to-noise ratio of Y, which is equal to $\langle Y\rangle/\sigma_Y$, is maximized when

$$\tilde{Q}(f) = N\frac{\gamma(f)}{P_1(f)P_2(f)f^3}, \tag{7}$$

where $\gamma(f)$ is the normalized overlap reduction function and P_i $(i = 1, 2)$ is the power spectrum density of the i-th detector's output. N is a normalization factor set so that $\langle Y\rangle = \Omega_{\rm gw}h_0^2T$:

$$N = \frac{20\pi^2}{3H_{100}^2}\left(\int_{-\infty}^{+\infty} df \frac{\gamma^2(|f|)}{f^6P_1(|f|)P_2(|f|)}\right)^{-1}. \tag{8}$$

If you want to know more details, see [7].

4.3. Main analysis

The process of the main analysis can be divided into four parts: data selection, calculation of the cross correlation, signal detection, and calculation of the upper limit. Before calculating the cross correlation, we have to remove the data which badly affects the result, such as glitches. Then, we decide whether a stochastic GW background is present or not according to the cross correlation value calculated with survived data. When it is judged that a stochastic GW background is absent, the upper limit on a stochastic GW background is calculated.

4.3.1. Data selection Ideally, the noise levels of the two detectors should be stationary through the whole observation. However, there are some glitches or non-stationary noise in the time series data, which will affect the result. Therefore we remove the data where the noise level is bigger.

First, the time series data is divided into several segments. (See figure 6.) Then, we remove the segments in which the data is noisy, and calculate the cross correlation only with the survived segments. We judge whether the data is noisy or not according to the whitened RMS in the frequency domain. However, when the analyzed frequency band is included in the calculation of the RMS, we may remove the segments in which a stochastic GW background is present, if the stochastic GW background is not stationary. Therefore, the analyzed frequency band should be relieved from the frequency band used as the indicator of the noise level.

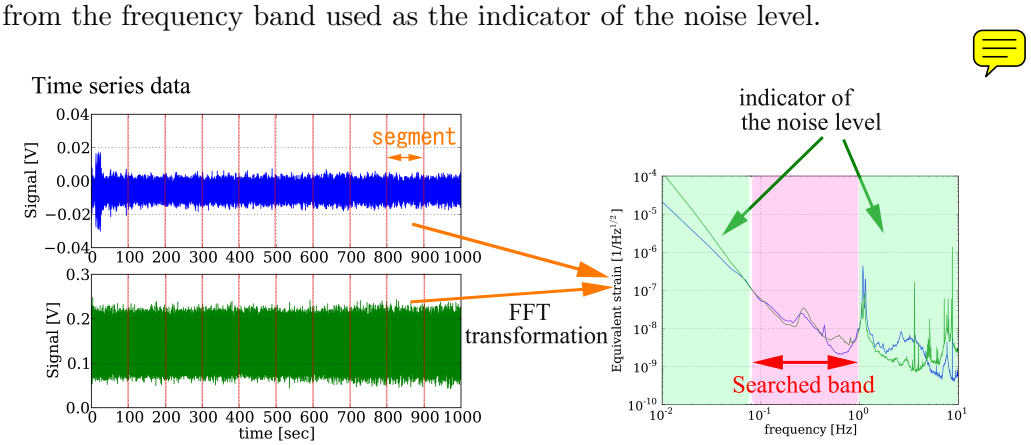

Figure 6. Data selection method

4.3.2. Calculating cross correlation The cross correlation value Ys are calculated with each survived segments according to the equation 6.

Here we restrict the analyzed frequency band, since the frequency band where the sensitivity is worse does not produces a good result. In order to decide the analyzed frequency band, we used the optimal filter $\tilde{Q}(f)$. The optimal filter is larger when the sensitivity to a stochastic GW background is better. Therefore, the frequency band where the optimal filter is biggest is chosen for the analyzed frequency band. (See figure 7)

4.3.3. Signal detection According to Ys calculated at each segments, we decide whether a stochastic GW background is present or not by the Neyman-Pearson criterion:

- if $\langle Y \rangle \geq z_\alpha$, a stochastic GW background is present.
- if $\langle Y \rangle < z_\alpha$, a stochastic GW background is absent.

Here, $\langle Y \rangle$ is the average of Ys calculated with the survived segments and α is the false alarm rate. This detection threshold z_α is set so that

$$\alpha = \int_{z_\alpha}^{+\infty} dy p(y|0), \tag{9}$$

where $p(y|0)$ is the probability distribution of $\langle Y \rangle$ when a stochastic GW background is absent.

In this case, we calculate the distribution of $\langle Y \rangle$ with time shifted data, which is considered to be relative to the probability distribution of $\langle Y \rangle$ when a stochastic GW background is absent. The distribution is shown in figure 8.

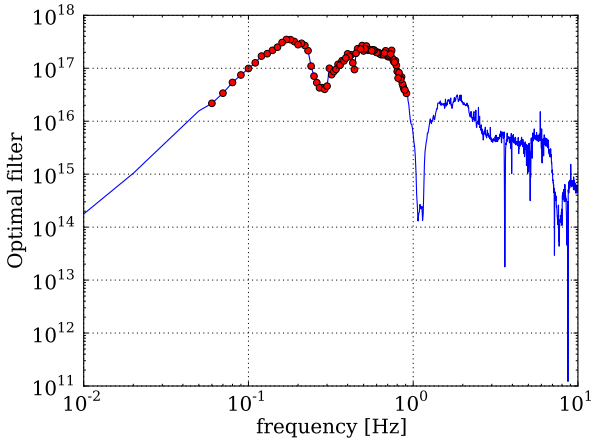

Figure 7. The blue line is the optimal filter. The red dots are the frequency bins which are chosen to be analyzed.

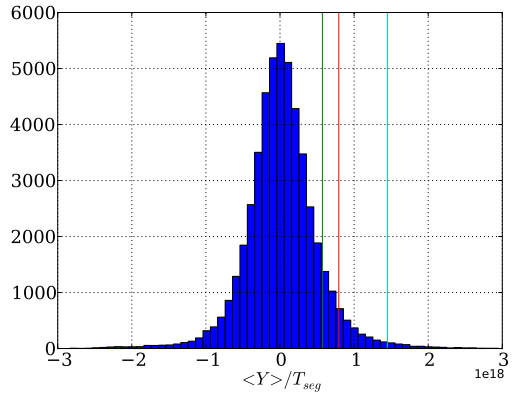

Figure 8. The distribution of $\langle Y \rangle$ with time shifted data. The sky blue, red, and green lines are the detection threshold z_α where $\alpha = 0.01, 0.05,$ and0.1 respectively.

4.3.4. Setting an upper limit When we cannot detect a stochastic GW background, we set an upper limit on a stochastic GW background. An upper limit means the amplitude of a stochastic GW background which we can detect if it would come to these detectors with the same noise levels.

In order to calculate it, we use the actual data set and mock signals. We make a mock signal of a stochastic GW background with a certain amplitude according to equation 3 (see figure 9), and inject it into the observational data. Then, we perform the same analysis described above with the injected data.

This process is repeated many times and we compute the rate at which we detect the mock signal, which is called detection efficiency. Figure 10 shows the detection efficiency at variable amplitude of a injected signals. The detection efficiency is equal to the confidence level to the upper limit. Therefore, for example, 95 % confidence upper limit is the amplitude of a mock signal at which the detection efficiency is 95 %.

4.4. Parameter tuning

In the process of the main analysis, there are some parameters whose optimal values depend on the data quality. Therefore, we performed pre-analysis and tuned these parameters. Here the

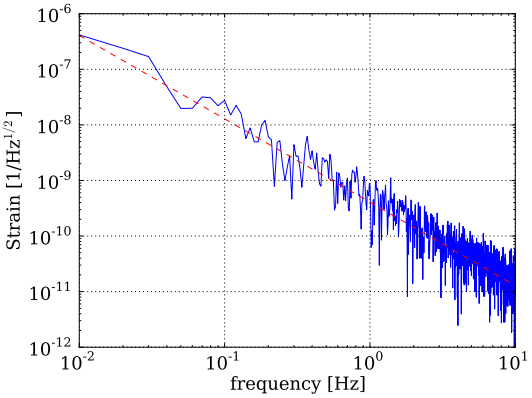

Figure 9. The strain of the mock signal of a stochastic GW background where $\Omega_{\rm gw}h_0^2 = 10^{18}$. It is basically a Gaussian noise, but it is multiplied by $f^{-3/2}$.

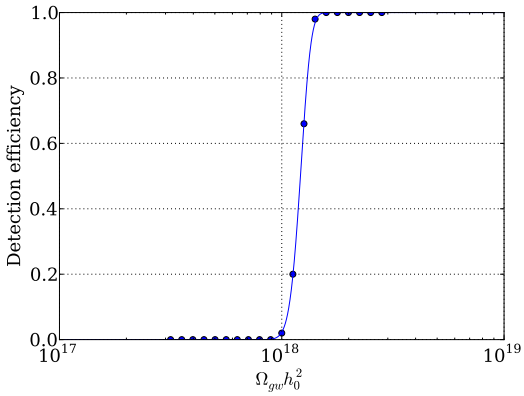

Figure 10. The detection efficiency. The blue dots are calculated probability and the blue line is an error function fitted to the blue dots.

time shifted data is used in order to prevent the result from being intentionally good.

The parameters to be tuned are the length of segments, the frequency band used as the indicator of the noise level at data selection, the amount of the segments which is removed, and the bandwidth of the analyzed frequencies.

Then, A flow chart of the whole analysis process is shown in figure 11.

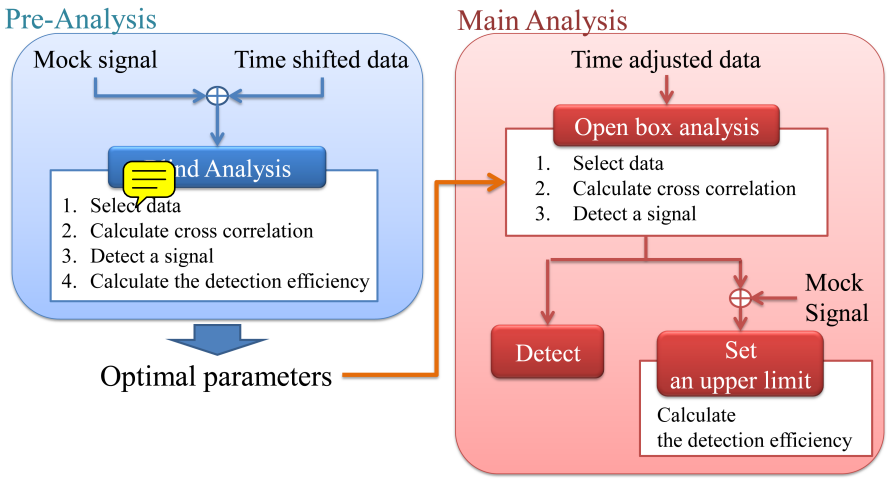

Figure 11. The flow chart of the analysis process.

5. Result

As a result of the parameter tuning, the length of the segment is set as 100 sec, i.e., the frequency resolution *df* is 0.01 Hz. We calculate RMS as the indicator of noise level at 0.01 – 0.05 and 1.0 – 10.0 Hz. Each 50 % of the segments are removed by the data selection, which results in about 14,000-second effective observation time. The analyzed frequency band is adjusted to 0.06 – 0.9 Hz. The width of searched frequency band is 0.85 Hz.

When the data is analyzed with these parameters, the detection threshold with false alarm rate 1 % for $\langle Y \rangle / T$ is $z_{0.01} = 1.2 \times 10^{19}$. And calculated $\langle Y \rangle / T$ with time adjusted data is -1.4×10^{17}, which is smaller than $z_{0.01}$. Therefore, we concluded that a stochastic GW background is absent. Moreover, we calculated that 95 % confidence upper limit with false alarm rate 1 % is $\Omega_{\rm gw} h_0^2 \leq 1.2 \times 10^{19}$.

This result is worse than the upper limit calculated with a single TOBA ~~by K. Ishidoshiro~~ [12]. It is considered to be because of a large seismic noise due to the earthquake occurred at May 11th, 2011. This observational run was started about 13 hours before the earthquake, and there were some foreshocks during the observation. Now we are planning to perform the simultaneous observational run again before long.

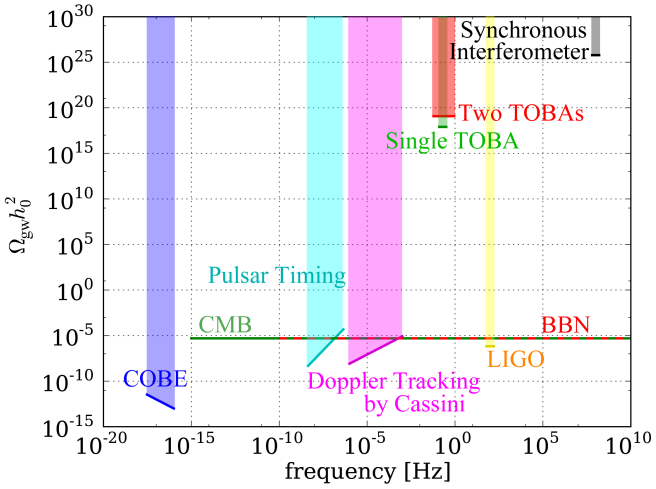

Figure 12. Upper limits established by TOBAs and other previous observations.

6. Summary and future plan

We searched a stochastic GW background with the prototypes of TOBA by the cross correlation method. TOBA is the novel GW detector whose advantage is that it has good sensitivity below 1 Hz unlike other ground-based detectors such as large interferometers. The prototype has 20-cm test mass bar, and levitated by the magnetic force of the superconductor and the magnet. Its sensitivity is $h \sim 10^{-8}$ at 0.3 Hz.

We demonstrated the simultaneous observational run and cross correlation analysis with two prototype TOBA at Tokyo and Kyoto, and established the system of the cross correlation analysis with TOBAs. As a redult of the analysis for detect a stochastic GW background, we cannot detect a stochastic GW background. Our 95% confidence upper limit is $\Omega_{\rm gw} h_-^2 \leq 1.2 \times 10^{19}$.

While we set a new upper limit at wider frequency band than previous result, this result is not good because the seismic noise is bigger than before. This is considered to be due to the fore-shocks due to the big earthquake occurred in Japan at May 11th, 2011. Therefore, we will perform the simultaneous observational run again. It is expected that we can derive a better result.

References

[1] Barish B C and Weiss R 1999 *Phys. Today* **52** 44

[2] Caron B *et al.* 1997 *Nucl. Phys. B* **54** 167
[3] Collaboration T L S and Collaboration T V 2009 *Nature* **460** 990
[4] Akutsu T *et al.* 2008 *Phys. Rev. Lett.* **101**(10) 101101
[5] Astone P *et al.* 1999 *Astron. Astrophys.* **351** 811
[6] Allen B 1996 (*Preprint* `gr-pc/9604033v3`)
[7] Maggiore M 2000
[8] Smith T L, Pierpaoli E and Kamionkowski M 2006 *Phys. Rev. Lett.* **97**(2) 021301
[9] Danzmann K 1997 *Class. Quantum Grav.* **14** 1399
[10] Kawamura S *et al.* 2006 *Class. Quantum Grav.* **23** 125
[11] Ando M *et al.* 2010 *Phys. Rev. Lett.* **105** 161101
[12] Ishidoshiro K *et al.* 2011 *Phys. Rev. Lett.* **106** 161101
[13] Ishidoshiro K 2009 *Search for low-frequency gravitational waves using a superconducting magnetically-levitated torsion antenna* Ph.D. thesis University of Tokyo
[14] Spergel D *et al.* 2003 *Astrophys. J. Suppl. Ser.* **148** 175
[15] Maggiore M 2008 *Gravitational Waves, Volume 1: Theory and Experiments* (Oxford University Press)